Current transport in nonpolar a-plane InN/GaN heterostructures Schottky junction

Mohana K. Rajpalke,[1] Thirumaleshwara N. Bhat,[1] Basanta Roul,[1,2] Mahesh Kumar,[1,2] and S. B. Krupanidhi[1,a)]
[1]*Materials Research Centre, Indian Institute of Science, Bangalore 560012, India*
[2]*Central Research Laboratory, Bharat Electronics, Bangalore 560013, India*

(Received 3 January 2012; accepted 27 June 2012; published online 24 July 2012)

The temperature dependent current transport properties of nonpolar a-plane $(11\bar{2}0)$ InN/GaN heterostructure Schottky junction were investigated. The barrier height (φ_b) and ideally factor (η) estimated from the thermionic emission (TE) model were found to be temperature dependent in nature. The conventional Richardson plot of the $\ln(I_s/T^2)$ versus 1/kT has two regions: the first region (150–300 K) and the second region (350–500 K). The values of Richardson constant (A^*) obtained from this plot are found to be lower than the theoretical value of n-type GaN. The variation in the barrier heights was explained by a double Gaussian distribution with mean barrier height values ($\overline{\varphi_b}$) of 1.17 and 0.69 eV with standard deviation (σ_s) of 0.17 and 0.098 V, respectively. The modified Richardson plot in the temperature range 350–500 K gives the Richardson constant which is close to the theoretical value of n-type GaN. Hence, the current mechanism is explained by TE by assuming the Gaussian distribution of barrier height. At low temperature 150–300 K, the absence of temperature dependent tunneling parameters indicates the tunneling assisted current transport mechanism. © *2012 American Institute of Physics*. [http://dx.doi.org/10.1063/1.4739261]

I. INTRODUCTION

It is becoming crucial to understand the Schottky barrier formation based on the GaN related materials, from a fundamental point of view as well as forming robust Schottky diodes.[1,2] The physical properties of GaN and related materials make it suitable for high power devices.[3] Iucolano *et al.*[4] reported the fabrication of Pt based Schottky diodes on c-plane GaN. Kim *et al.*[5] reported the Pd Schottky diodes grown on c-plane GaN, with higher barrier height compared to Pd Schottky diodes grown on a-plane GaN. Such variation is explained by the absence of polarization-induced surface charges for the a-plane GaN sample as compared to that of the *c*-plane sample. Phark *et al.*[6,7] reported the temperature dependent current transport in Pt Schottky contact to a-plane GaN. The Pt and Au based polar c-plane GaN Schottky diodes with higher barrier heights compare to the nonpolar a-plane GaN have been discussed in the previous report.[8] The Schottky barrier height (SBH) is a measure of the mismatch of the energy levels for the majority carriers across the semiconductor heterostructures or metal/semiconductor interfaces. The large difference between the band gaps of InN and GaN suggests the existence of Schottky barrier at InN/GaN interface. Chen *et al.*[9] reported transport studies on c-plane InN/GaN Schottky interfaces. Roul *et al.*[10] reported the temperature dependent barrier heights in polar c-plane InN/GaN Schottky diodes. However, there is no report on the transport behaviour of nonpolar a-plane $(11\bar{2}0)$ InN/GaN heterostructure interfaces.

The temperature dependence of the I-V characteristics of the Schottky diodes gives the detailed information about the nature of barrier formation at the interface and their conduction process.[11] Usually, the thermionic emission (TE) mechanism is used to extract the Schottky barrier height and the value of the ideality factor (n) which is expected to be close to unity. However, the experimental I–V–T data obtained for many different Schottky diodes often exhibit non-ideal I–V–T characteristics and show temperature dependent barrier height and ideality factor.[11–13] These changes are more pronounced particularly at low temperatures, which leads to nonlinearity in the activation energy plot of $\ln(I_s/T^2)$ versus $1/kT$. Such behavior is usually interpreted by the existence of inhomogeneities at the interface, possibly due to doping inhomogeneities and defects at the interfaces.[14–17] Mamor *et al.*[14] reported the lateral inhomogeneity of the SBH which is attributed to the presence of defects in the GaN film. Ravinandan *et al.*[18] studied the Pt/Au Schottky contacts on n-type GaN in the temperature range of 85–405 K and reported increase in zero-barrier heights (φ_b) with temperature. Dogan *et al.*[19] reported the temperature dependent current–voltage (I–V) characteristics of Au/Ni/n-GaN Schottky diodes and explained the behaviour using TE model, with the help of barrier inhomogeneity at metal/GaN interface.

In this work, we have performed the temperature dependent transport studies of nonpolar a-plane InN/GaN heterostructure Schottky diode grown by plasma assisted molecular beam epitaxy (PAMBE). The thermionic emission with Gaussian distribution was used to investigate the anomalous variation of barrier height and ideal factor with temperature.

a)Author to whom correspondence should be addressed. Electronic mail: sbk@mrc.iisc.ernet.in.

II. EXPERIMENTAL PROCEDURE

Nonpolar a-plane $(11\bar{2}0)$ InN/GaN (~200 nm/200 nm) heterostructures were grown on r-sapphire substrate by Omicron Nanotechnology plasma assisted molecular beam epitaxy (MBE) system. Sapphire substrates were degreased using trichloroethylene and etched using H_2SO_4:H_3PO_4 (3:1) at 150 °C for 20 min and rinsed with deionized water before loading into the molecular-beam epitaxy chamber. Thermal cleaning was done at 850 °C inside MBE chamber for 30 min under ultra high vacuum (MBE pressure $\sim 1 \times 10^{-10}$ mbar). Low temperature GaN buffer layer of thickness 20 nm was grown at 500 °C followed by GaN epilayer growth at 760 °C. Finally, low temperature InN buffer layer (~20 nm) was grown at 400 °C followed by InN epilayer (~180 nm) growth at 500 °C temperature. During growth, the nitrogen pressure was kept at 2.8×10^{-5} mbar, corresponding to the nitrogen flow rate of 0.5 sccm and the forward RF-power of the plasma source was kept at 350 W. The structural characterization of the film was carried out by reflection high energy electron reflection (RHEED) and high resolution x-ray diffraction (HRXRD) measurements using a Bruker-D8 discover diffractometer. Ecopia HMS-5000 Hall-effect measurement system was used to determine the carrier concentration of undoped n-type a-plane GaN. The carrier concentration of nonpolar a-plane GaN layer was found to be 5.1×10^{17} cm^{-3} at room temperature. The area of the junction between InN and GaN is 4×10^{-2} cm^2. The two aluminium (Al) metal contacts (ohmic) were fabricated to the InN and GaN. The I-V measurements were carried out by using computer interfaced Keithley-236 source meter system in the temperature range of 150-500 K by steps of 50 K.

III. RESULTS AND DISCUSSION

Fig. 1 shows 2θ-ω scan of nonpolar a-plane $(11\bar{2}0)$ InN/GaN heterostructures grown on r-plane $(1\bar{1}02)$ sapphire substrate. The peak at 57.7° and 51.61° are assigned to the a-plane $(11\bar{2}0)$ GaN and a-plane $(11\bar{2}0)$ InN reflections, respectively, along with that from the r-plane sapphire substrate. Figures 2(a) and 2(b) show the RHEED patterns in the azimuths [0001] for a-plane GaN and a-plane InN, respectively. The Bragg spots appear with weak streaky lines in the RHEED patterns observed for a-plane GaN confirms the reasonable smooth surface. Spotty nature of a-plane InN RHEED pattern indicating the 3D growth of nonpolar a-plane InN.

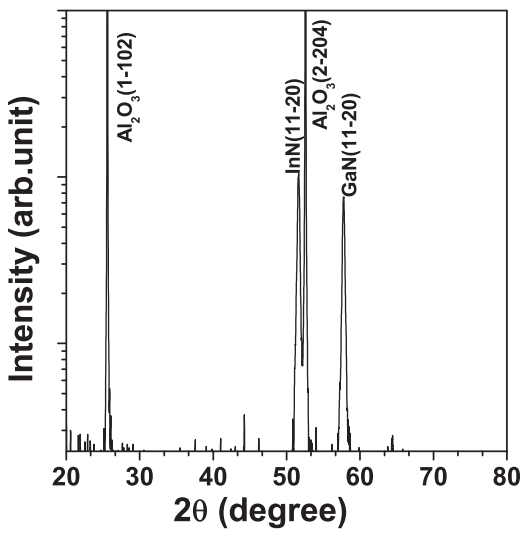

FIG. 1. 2θ-ω HRXRD scan of nonpolar a-plane InN/GaN heterostructures grown on r-sapphire substrate.

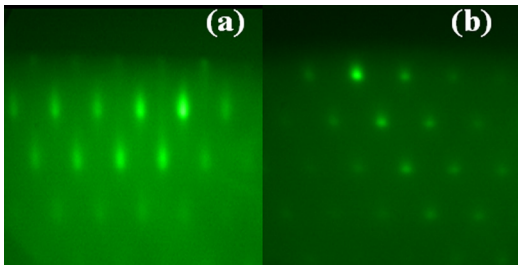

FIG. 2. RHEED patterns of (a) a-plane (11-20) GaN (b) a-plane (11-20) InN taken along (0 0 0 1) azimuth.

Fig. 3 shows the room temperature I-V characteristic curve of nonpolar a-plane InN/GaN heterostructure Schottky diode. The inset figure shows the schematic diagram of the device. The rectifying behaviour of the I-V curve indicates the existence of Schottky barrier at the InN and GaN interface. The forward current-voltage (I-V) characteristics of the nonpolar a-plane $(11\bar{2}0)$ InN/GaN heterostructure in the temperature range of 150-500 K are shown in Fig. 4. The values of Schottky barrier height (φ_b) and the ideality factor (η) for the junction were calculated as a function of measuring temperature and by fitting the linear region of the forward I-V curves using the thermionic model (TE) model. From the TE theory, where $qV > 3kT$, the relation between current and applied bias voltage for the Schottky diode is given by[20,21]

$$I = I_s \exp\left(\frac{qV}{\eta kT}\right), \tag{1}$$

where

$$I_s = AA^*T^2 \exp\left(-\frac{\varphi_b}{kT}\right). \tag{2}$$

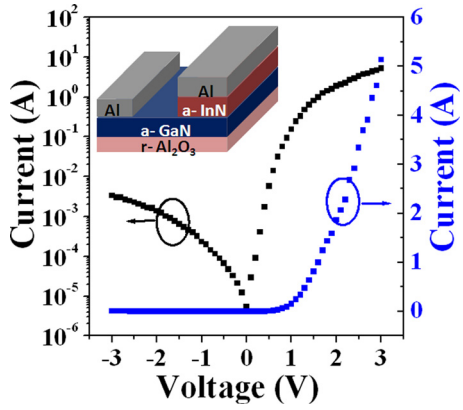

FIG. 3. The room temperature I-V characteristics of the nonpolar a-plane InN/GaN Schottky junction. The inset shows the schematic diagram of the nonpolar a-plane InN/GaN heterojunction.

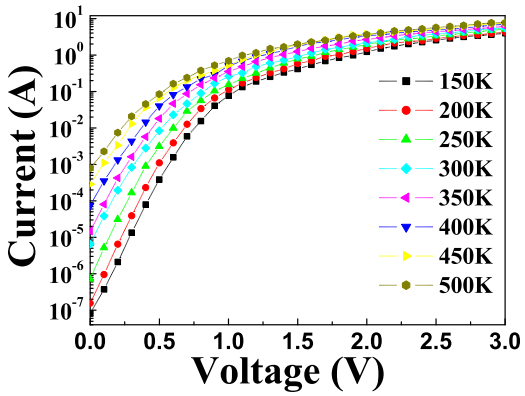

FIG. 4. The temperature dependent forward I-V characteristics for the nonpolar a-plane InN/GaN Schottky junction.

Here, I_s is the saturation current density, T is the measurement temperature, A is the contact area, A^* is the Richardson's constant, k is the Boltzmann constant, q is the electron charge, φ_b is the Schottky barrier height, and η is the ideality factor. The theoretical value of A^* was assumed to be 24 A cm^{-2} K^{-2}.[20] The values of φ_b and η at different temperatures were obtained from the linear region of the forward I-V characteristics by fitting Eq. (1) as shown in Fig. 5. The temperature dependent variation has been observed for both φ_b and η, i.e., φ_b increases and η decreases with increasing temperature. We found n and φ_b values ranging from 1.65 and 0.83 eV (500 K) to 4.1 and 0.4 eV (150 K), respectively. Thus, the temperature dependence of φ_b indicates the inhomogeneous nature of InN/GaN interface. Our earlier report on polar c-plane InN/GaN heterostructures also shows the inhomogeneous barrier height.[10] The inhomogeneous SBH may arise due to the various types of defects present at the InN/GaN interface.[15,17] Kim *et al.*[22] observed the temperature dependent barrier height and ideality factor in Pt/a-plane GaN Schottky diode and the observed inhomogeneity were explained in terms of surface defects in nonpolar a-plane GaN.

In order to evaluate the barrier height (φ_b), Richardson plot of saturation current has been used. Equation (2) can be rewritten as

$$\ln\left(\frac{I_s}{T^2}\right) = \ln(AA^*) - \frac{q\varphi_b}{kT}. \tag{3}$$

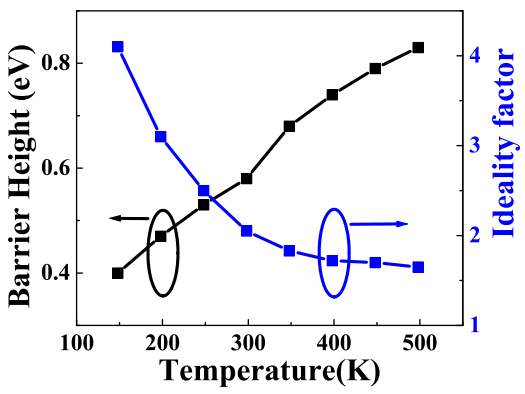

FIG. 5. The temperature dependent variation of barrier height with the ideality factor.

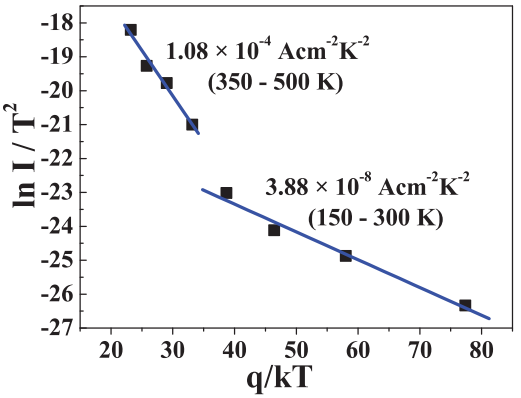

FIG. 6. The conventional Richardson's plot of $\ln(I_s/T^2)$ versus $1/kT$.

Fig. 6 shows the temperature dependent $\ln(I_s/T^2)$ versus $1/kT$ plot in the temperature range of 150 K–500 K. The two linear regions have been observed in the temperature region 150 K–300 K and 350 K–500 K. The fitting of these two regions reveals the values of Richardson's constant (A^*) and barrier height (φ_b), which were found to be 1.08×10^{-4} A cm^{-2} K^{-2} and 0.27 eV for the first region (350 K–500 K) and 3.88×10^{-8} A cm^{-2} K^{-2} and 0.08 eV for the second region (150 K–300 K), respectively. The calculated values of Richardson constant (A^*) are much lower than the theoretical value of 24 A cm^{-2} K^{-2} for n-GaN. The deviation of Richardson plot indicates the inhomogeneous barrier heights and potential fluctuations at the interface, which consist of low and high barrier areas.[23–25] At low temperature the carriers are able to surmount the lower barriers and as the temperature increases the carriers have sufficient energy to surmount the higher barrier at the InN/GaN interface, thereby increase in the measured barrier height with increasing the temperature.

The inhomogeneous nature of Schottky barrier at the InN/GaN interface can be explained by considering the Gaussian distribution of barrier height, which can be written as[26,27]

$$P(\varphi_b) = \frac{1}{\sigma_s\sqrt{2\pi}}\exp\left[-\frac{(\varphi_b - \overline{\varphi_b})^2}{2{\sigma_s}^2}\right], \tag{4}$$

where $1/\sigma_s\sqrt{2\pi}$ is the normalization constant and $\overline{\varphi_b}$ and σ_s are the mean and standard deviation of barrier height, respectively. The effective barrier height, φ_b given by the expression,

$$\varphi_b = \overline{\varphi_b} - \frac{q\sigma^2}{2kT}, \tag{5}$$

where $\overline{\varphi_b}$ is the zero bias mean barrier height and σ_s is the standard deviation which are linearly bias dependent on Gaussian parameters.

Fig. 7 shows the φ_b verses q/2kT plots. From Fig. 7, the straight line whose intercept point is equal to the zero bias mean barrier height ($\overline{\varphi_b}$) and the slope gives the standard deviation (σ_s), which measure the extent of inhomogeneities present at the interface. Fig. 7 shows two linear regions

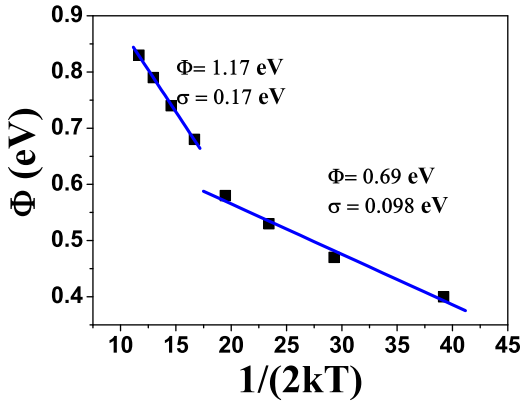

FIG. 7. Plot of φ_{ap} versus q/2kT.

indicating the existence of double Gaussian distribution of barrier height at the InN/GaN interface. The intercept and slopes of these straight lines give two sets of values of $\overline{\varphi_b}$ and σ_s as 1.17 eV and 0.17 V in the temperature range of 350–500 K and 0.69 eV and 0.098 V in the temperature range of 150–300 K, respectively.

Due to the barrier height inhomogeneities, the conventional Richardson plot is modified, which is given by

$$\ln\left(\frac{I_s}{T^2}\right) - \left(\frac{q^2\sigma^2}{2k^2T^2}\right) = \ln(AA^*) - \frac{q\overline{\varphi_b}}{kT}. \quad (6)$$

Fig. 8 shows the modified $\ln(I_s/T^2)$-$q^2\sigma^2/2k^2T^2$ versus q/kT plots. From Fig. 8, the intercept point determines the value of AA^* and the slope gives the zero bias mean barrier height ($\overline{\varphi_b}$). Thus, the $\ln(I_s/T^2)$-$q^2\sigma^2/2k^2T^2$ values were calculated for both two values of σ_s obtained in the temperature ranges of 150–300 K and 350–500 K. In the first region (300–500 K), the values of the zero bias mean BH ($\overline{\varphi_b}$) and effective Richardson constant (A*) were obtained from the slope and intercept of this straight line found to be 1.15 eV and 19.5 A/cm^2 K^2, respectively. The obtained Richardson constant in the temperature range of 350–500 K is very close to the theoretical value of 24 A/cm^2 K^2 for n-type GaN. For polar c-plane InN/GaN, the value of BH ($\overline{\varphi_b}$) and effective Richardson constant (A*) were found to be 1.6 eV and 25.8 A/cm^2 K^2, respectively.[10] The barrier height of nonpolar a-plane InN/GaN (1.15 eV) found to be lesser compared to c-plane InN/GaN (1.6 eV)

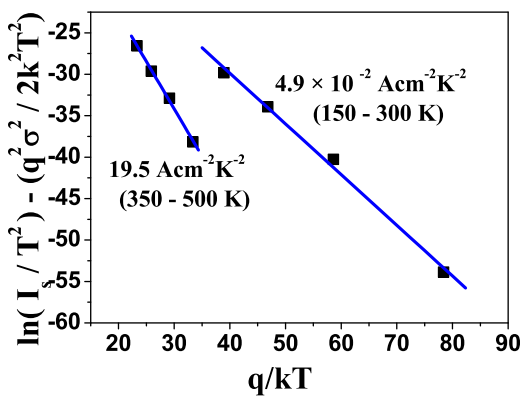

FIG. 8. Modified Richardson plot of $\ln(I_s/T^2) - q^2\sigma^2/2k^2T^2$ versus q/kT.

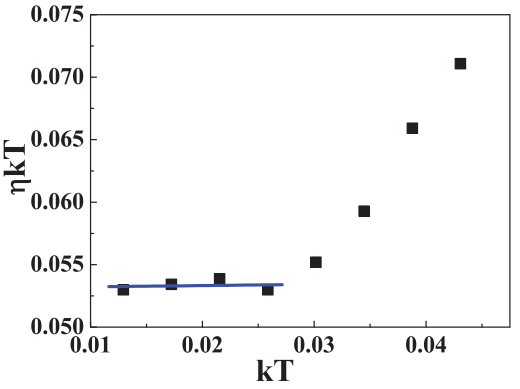

FIG. 9. Plot of nk_BT as a function of k_BT.

heterostructures. The reduced barrier height in nonpolar a-plane InN/GaN with respect to the polar c-plane InN/GaN could be explained in terms of absence of polarization field at the interface.

In the second region (150–300 K), the values of the zero bias mean BH ($\overline{\varphi_b}$) and Richardson constant are 0.62 eV and 4.9×10^{-2} A/cm^2 K^2, respectively. The large deviation of A^* in the temperature range of 150–300 K indicates that the TE mechanism does not dominates in the low temperature (150–300 K). Fig. 9 shows $E_0 = \eta kT$ versus kT plot for the nonpolar a-InN/GaN Schottky diode in the temperature range of 150–500 K. When the thermionic field emission (TFE) model or field emission (FE) model controls the current transport, the forwardbias currents are given by[28]

$$I = I_0 \exp\left(\frac{qV}{E_0}\right), \quad (7)$$

where

$$E_0 = E_{00} \coth\left(\frac{E_{00}}{kT}\right) = \eta kT. \quad (8)$$

From Fig. 9, one can see that the value of E_0 is independent of temperature at the low temperature (150–300 K). If the FE dominates, then the E_0 will lie on straight line.[29] In this case, E_0 is independent of temperature and $E_0 = E_{00}$.[30] As seen from the figure, $E_0 = E_{00}$ was obtained 53 meV. The relatively large E_{00} values compared to the kT values in the temperature of 150–300 K indicate that the tunneling current is a dominant component at low temperature. The possible origin of the high characteristics energy or the FE current transport may be attributed to the accumulation of a large amount of defect states near the InN/GaN interface. At low temperatures, carrier does not have enough energy to surmount the barrier. Hence, it will tunnel through the defects at the interface. At higher temperature (350–500 K), the carriers have enough energy to surmount the barrier and current transport is dominated by TE mechanism.

IV. CONCLUSION

The forward bias I-V characteristics of the nonpolar a-plane $(11\bar{2}0)$ InN/GaN heterostructure were measured in the temperature range of 150-500 K. The measured values of

barrier height and ideal factor from the TE model show the temperature dependent variation. The anomalous behavior has been explained in terms of inhomogeneous Schottky barrier and could be attributed to the InN/GaN heterostructure interfacial defects causing local variation of the Schottky barrier height. The double Gaussian distribution has mean barrier height values ($\overline{\varphi_b}$) of 1.17 and 0.69 eV with standard deviation (σ_s) of 0.17 and 0.098 V, respectively. The modified Richardson $\ln(I_s/T^2) - q^2\sigma^2/2k^2T^2$ versus q/kT plot in the temperature range of 350–500 K yielded the Richardson constant of 19.5 $A/cm^2\ K^2$ which is very close to the theoretical value of 24 $A/cm^2\ K^2$ for n-type GaN, indicating that the TE model with a Gaussian distribution of barrier heights could explain the experimental data. The temperature independent nature of tunneling parameters E_0 at low temperature range (150–300 K) indicates that the current is dominated by the tunneling assisted mechanisms.

[1]A. R. Arehart, B. Moran, J. S. Speck, U. K. Mishra, S. P. DenBaars, and S. A. Ringel, J. Appl. Phys. **100**, 023709 (2006).
[2]K. Cinar, N. Yildirim, C. Coskun, and A. Turut, J. Appl. Phys. **106**, 073717 (2009).
[3]H. W. Seo, L. W. Tu, Q. Y. Chen, C. Y. Ho, Y. T. Lin, K. L. Wu, D. J. Jang, D. P. Norman, and N. J. Ho, Appl. Phys. Lett. **96**, 101114 (2010).
[4]F. Iucolano, F. Rocaforte, F. Giannzzo, and V. Raineri, J. Appl. Phys. **102**, 113701 (2007).
[5]H. Kim, S. N. Lee, Y. Park, J. S. Kwak, and T.-Y. Seong, Appl. Phys. Lett. **93**, 032105 (2008).
[6]S. H. Phark, H. Kim, K. M. Song, P. G. Kang, H. S. Shin, and D. W. Kim, J. Phys. D: Appl. Phys. **43**, 165102 (2010).
[7]S. H. Phark, H. Kim, K. M. Song, and D. W. Kim, J. Korean Phys. Soc. **58**, 1356 (2011).
[8]H. Kim, S. H. Phark, K. M. Song, and D. W. Kim, J. Korean Phys. Soc. **60**, 104 (2012).
[9]N. C. Chen, P. H. Chang, Y. N. Wang, H. C. Peng, W. C. Lien, C. F. Shih, C.-A. Chang, and G. M. Wu, Appl. Phys. Lett. **87**, 212111 (2005).
[10]B. Roul, T. N. Bhat, M. Kumar, M. K. Rajpalke, N. Sinha, A. T. Kalghatgi, and S. B. Krupanidhi, Solid State Commun. **151**, 1420 (2011).
[11]I. Taşçıoğlu, U. Aydemir, and Ş. Altındal, J. Appl. Phys. **108**, 064506 (2010).
[12]O. Pakma, N. Serin, T. Serin, and Ş. Altındal, J. Appl. Phys. **104**, 014501 (2008).
[13]Y. Jung, M. Mastro, J. Hite, C. R. Eddy, Jr., J. Kim, Thin Solid Films **518**, 1747 (2010).
[14]M. H. Mamor, J. Phys.: Condens. Matter. **21**, 335802 (2009).
[15]A. Hattab, J. L. Perrossier, F. Meyer, M. Barthula, H. J. Osten, and J. Griesche, Mater. Sci. Eng. B. **89**, 284 (2002).
[16]K. Wang, C. Lian, N. Su, D. Jena, and J. Timler, Appl. Phys. Lett. **91**, 232117 (2007).
[17]F. E. Cimilli, M. Saglam, and A. Turut, Semicond. Sci. Technol. **22**, 851 (2007).
[18]M. Ravinandan, P. Koteswara Rao, and V. Rajagopal Reddy, J. Optoelectron. Adv. Mater. **10**, 2787 (2008).
[19]S. Dogan, S. Duman, B. Gurbulak, S. Tuzemen, and H. Morkoc, Physica E **41**, 646 (2009).
[20]L. Wang, M. I. Nathan, T. Lim, M. A. Khan, and Q. Chen, Appl. Phys. Lett. **68**, 1267 (1996).
[21]H. Morkoc, *Handbook of Nitride Semiconductors and Devices* (Wiley-VCH, 2008).
[22]H. Kim, S. H. Phark, K. M. Song, and D. W. Kim, AIP Conf. Proc. **1399**, 923 (2011).
[23]F. E. Cimilli, M. Sağlam, H. Efeoğlu, and A. Türüt, Physica B **404**, 1558 (2009).
[24]R. T. Tung, J. Appl. Phys. **88**, 7366 (2000).
[25]R. T. Tung, Phys. Rev. B **45**, 13509 (1992).
[26]A. Singh, Solid-State Electron. **28**, 223 (1993).
[27]P. G. McCafferty, A. Sellai, P. Dawson, and H. Elabd, Solid-State Electron. **39**, 583 (1996).
[28]E. H. Rhoderick and R. H. Williams, *Metal-Semiconductor Contacts*, 2nd ed. (Clarendon, Oxford, 1988).
[29]E. Arslan, S. Altındal, S. Ozcelik, and E. Ozbay, Semicond. Sci. Technol. **24**, 075003 (2009).
[30]A. Y. C. Yu and E. H. Snow, J. Appl. Phys. **39**, 3008 (1968).